

Supporting information for:

**Coexistence of chiral hydrophilic and achiral hydrophobic
channels in one multi-helical-array metal-organic framework
embodying helical water cluster chains**

Shuangquan Zang, Yang Su, Chunying Duan, Yizhi Li, Huizhen Zhu, Qingjin Meng*

Coordination Chemistry Institute and the State Key Laboratory of Coordination Chemistry,
School of Chemistry and Chemical Engineering, Nanjing University,
Nanjing 210093, P. R. China

*Corresponding Author: *Qingjin Meng*
Telephone number: (86)-25-83597266
Fax number: (86)-25-83314502
Email address: mengqj@nju.edu.cn

Table S1. Hydrogen bonds associated with the helical water cluster chain, distances (\AA) and angles ($^\circ$).

D-H	d(D-H)	d(H \cdots A)	\angle DHA	d(D \cdots A)	A
O(26)-H(26B)	0.92(8)	1.94(8)	156(6)	2.806(6)	O(28) ^a
O(27)-H(27B)	0.92(8)	2.00(8)	153(7)	2.857(6)	O(26)
O(28)-H(28B)	0.91(7)	1.92(7)	164(6)	2.804(7)	O(27)
O(29)-H(29A)	0.91(8)	2.19(8)	163(6)	3.079(6)	O(28) ^b
O(30)-H(30A)	0.91(8)	2.19(8)	170(7)	3.093(6)	O(29)
O(27)-H(27A)	0.92(8)	2.30(8)	147(6)	3.120(7)	O(30) ^c
O(20)-H(20C)	0.90	1.91	158.7	2.769(6)	O(29) ^d

Symmetry code: ^a -y+3/4, x+1/4, z+1/4; ^b x, y, z-1; ^c y-1/4, -x+3/4, z+3/4; ^d -x+1/2, -y+1, z+1/2.

Table S2. Other hydrogen bonds in **1**, distances (\AA) and angles ($^\circ$). (D, donor atom; A, acceptor atom).

D-H	d(D-H)	d(H \cdots A)	\angle DHA	d(D \cdots A)	A
O(18)-H(18B)	0.90	2.24	115.2	2.749(6)	O(3)
O(20)-H(20B)	0.90	1.86	162.7	2.735(6)	O(7)
O(21)-H(21C)	0.90	2.16	118.8	2.716(7)	O(10)
O(21)-H(21C)	0.90	2.56	140.1	3.298(6)	O(12)
O(24)-H(24C)	0.90	2.34	165.6	3.220(6)	O(11)
O(24)-H(24C)	0.90	2.35	119.9	2.910(6)	O(22)
O(17)-H(17B)	0.90	2.15	129.3	2.806(6)	O(16) ^c
O(18)-H(18B)	0.90	2.64	163.3	3.508(6)	O(23) ^b
O(19)-H(19B)	0.90	2.27	110.6	2.721(6)	O(13) ^d
O(22)-H(22A)	0.90	1.73	160.0	2.599(6)	O(14) ^e
O(22)-H(22C)	0.90	1.96	155.3	2.806(5)	O(9) ^e
O(23)-H(23A)	0.90	2.27	152.8	3.100(6)	O(13) ^f
O(23)-H(23A)	0.90	2.30	116.4	2.814(6)	O(16) ^f
O(23)-H(23A)	0.90	2.59	113.5	3.060(6)	O(17) ^a
O(23)-H(23B)	0.90	2.02	114.6	2.532(7)	O(3) ^a
O(24)-H(24B)	0.90	1.96	156.2	2.803(7)	O(11) ^e

Symmetry codes: ^a -y+3/4, x+1/4, z+1/4; ^b y-1/4, -x+3/4, z-1/4; ^c -y+5/4, x+1/4, -z+1/4; ^d y-1/4, -x+3/4, z+3/4; ^e -x+1/2, -y+3/2, -z+1/2; ^f x, y, z+1.

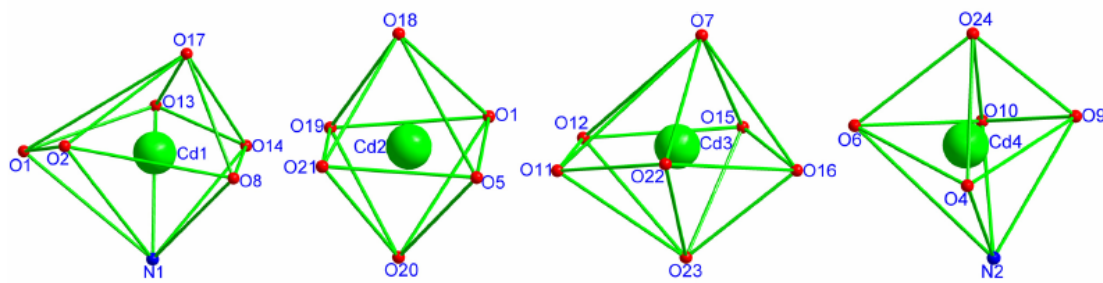


Fig. S1 The polyhedron representation of coordination environments for Cd1, Cd2, Cd3, and Cd4 atoms

The Cd1 ion (mode **1**, Scheme 1) is seven-coordinate and is described as a distorted pentagonal-bipyramidal geometry with one long axis (Cd1-O1 = 2.826 Å) (Fig. S1): Four oxygen atoms from 2-COO⁻ (mode **1**) and 2'-COO⁻ (mode **2**) in bichelating fashion, one oxygen atom from 3'-COO⁻ in mode **1**, one nitrogen atom from bpy as well as one terminal water molecular. The coordination geometry for the six-coordinate Cd2 ion (mode **I** in Scheme 1) is close to that of an octahedral (Figure S1): Two oxygen atoms from 2- and 2'-positioned carboxylate groups of one bpta ligand in mode **I** and four water molecules. The Cd3 ion (Scheme 1 and Fig. 1) is seven-coordinate and is described as a pentagonal-bipyramidal geometry: Four oxygen atoms from 3- and 3'-positioned carboxylate groups of two bpta moieties in bichelating fashion in mode **II**, one oxygen atom from 3'-positioned carboxylate groups in mode **I**, and two terminal water molecules. The Cd4 ion is six-coordinate and is described as an octahedral geometry (Fig. 1 and S1): One oxygen atom from 2'-positioned carboxylate groups in mode **I**, two oxygen atoms from 2-positioned carboxylate groups in bichelating fashion in mode **II**, one nitrogen from bpy, and two water molecules.

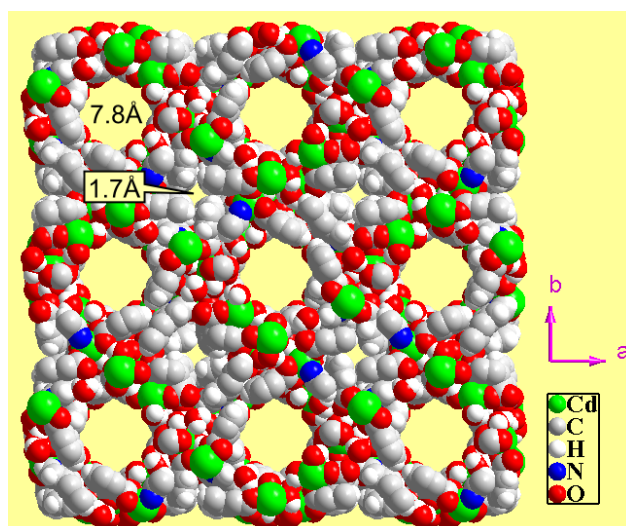


Fig. S2 Space-filling model of **1** indicating two distinct types of channels. Van der Waals radii are excluded when calculating the channel diameters.

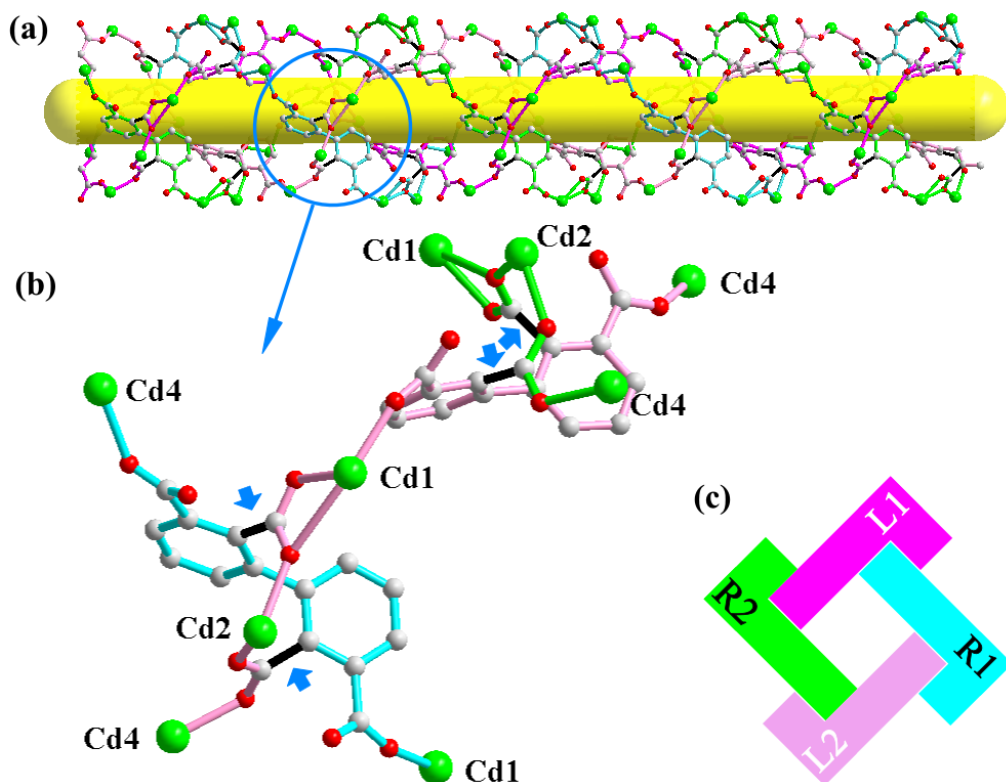


Fig. S3 (a), The achiral small channel (coordinated waters and bpy molecules are omitted for clarity). Two right-handed chains are marked cyan and green, while two left-handed chains are marked magenta and pink (b), The pink chain (showing the smallest repeat unit) crosses over the cyan chain and passes under the green chain. Black bonds (pointed by small bold arrows) are places where chains with opposite orientations are connected (c), A conceptual representation of the interweaving of the four chains. Every L-shaped symbol stands for a single chain (R = right handedness, L = left handedness). Each chain crosses over (the short arm) and passes under (the long arm) two chains with the opposite orientation.

The formation of this unit can be seen as two steps: Cd4 and Cd1 ions are firstly bridged together through 2- and 2'-positioned carboxylate groups in mode I in one arrangement and pass through Cd2 ions; Then, they are further united together through 3- and 3'-positioned carboxylate groups in mode I in another arrangement and pass through bptc ligand (Fig. S3).

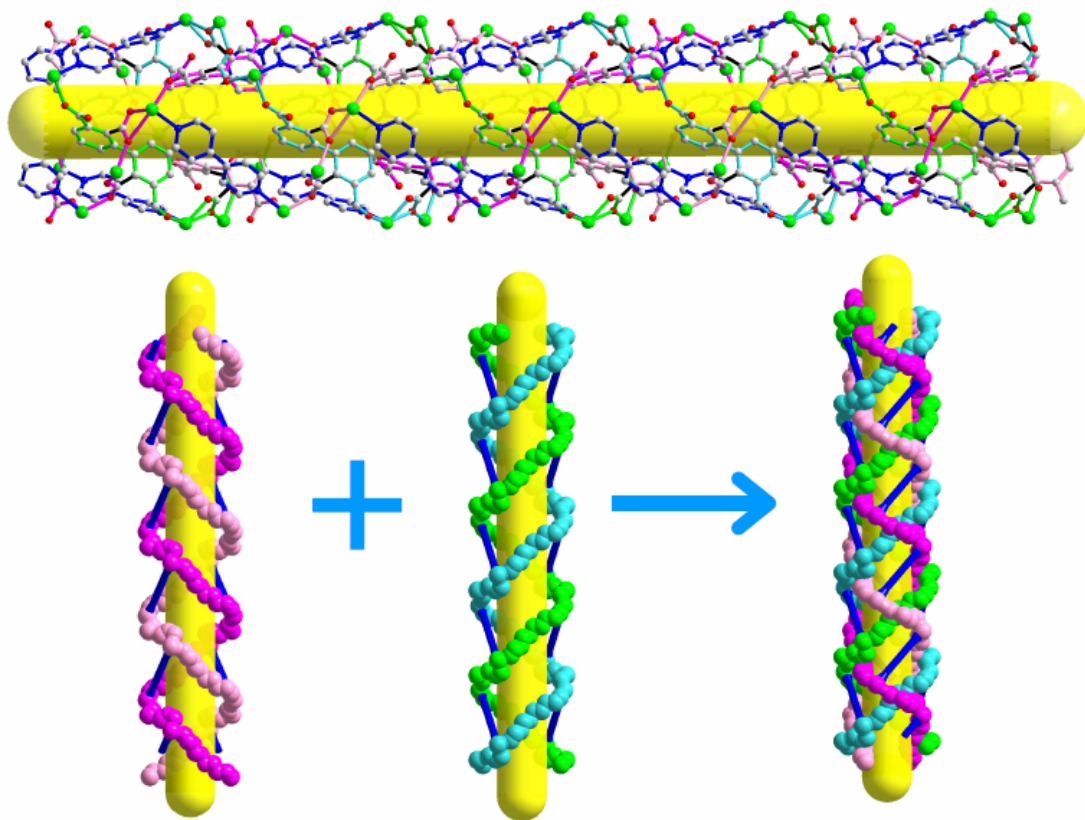


Fig. S4 Top: view of the small achiral channel. Two right-handed chains are marked cyan and green, while two left-handed chains are marked magenta and pink. bpy molecules are marked blue. Bottom: The space filling representation of interwoven two double-stranded helical ribbons with opposite orientations. Helices with the same chirality are linked by the bpy molecules (represented as blue sticks).

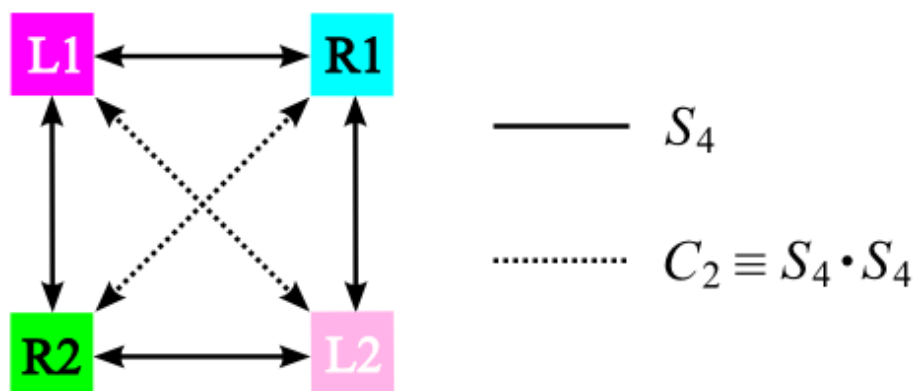


Fig. S5 The symmetry relationship of the four helical chains. R = right handedness; L = left handedness.

Helical chains with the same orientation are related by C_2 operations (a C_2 operation is equivalent to two successive S_4 operations), whereas helical chains with the opposite orientation are related by S_4

operations (Fig. S3 and S5).

Although *crystallographically* it is an S_4 -axis rather than a screw axis that passing through these four chains, each of these chains is indeed a helical chain in a *geometric* sense. For every chain, when rotating about the S_4 -axis through 180° and then translating along the S_4 -axis by c , it will be brought into self-coincidence, which exactly meets the geometric and symmetric requirements for a helical chain. Considering that the pitch of each chain is $2c$, if we chose $2c$ as the translational unit, then each chain could be brought into self-coincidence by successive a rotation through 180° and a translation by half of the unit, in accord with the definition of a crystallographic 2_1 -helix.

The absence of a screw axis can be explained as a symmetry issue in the crystallographic point of view. As we all know, helices of the left- and right-handedness are enantiomers and can only be related by symmetry elements that include reflections/inversions. S_4 -axis is such a symmetry element but screw axis is not. Now that the four helical chains having opposite orientations share a common axis, this axis must not be a screw axis according to the above symmetry constraint. Therefore the existence of helical chains does not conflict with the lack of a screw axis, and *vice versa*.

In the aspect of chemistry, this particular interesting situation is certainly a consequence of the unique twisted conformation of the bptc ligand and the coordination mode this ligand affords.

The above interpretation can also be exemplified by a simple geometric model as depicted in Figure S6. Let's start with a planar double-columned infinite ladder (Fig. S6a). For the purpose of comparison, the left and right rails are colored as magenta, the middle rail as pink, and the rungs as green and cyan alternatively. By rolling up this ladder around a proper axis, we can make the rungs link together end to end with their neighbors bearing the same color, affording two chains of green and cyan correspondingly. At the same time, the left and right rails are completely coincided and afford a single magenta chain in addition to the pink one from the middle rail (Fig. S6g). The rolling axis is just the S_4 -axis passing through the resulting structure. It can be strictly proved that these four chains are all helical chains with two of them left-handed (magenta and pink) and the other two right-handed (green and cyan). To all appearances, this structure is an analogue to the four chains comprising the small channel (Fig. S6h).

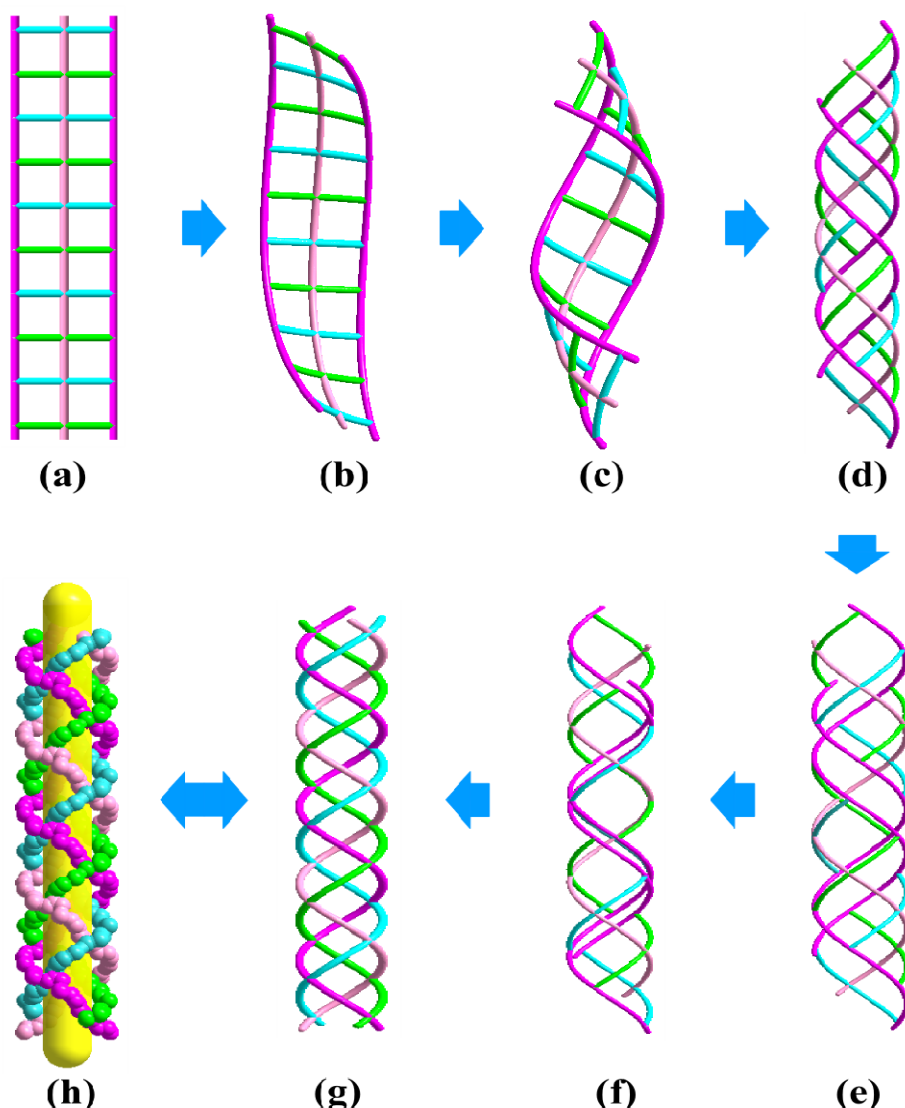


Fig. S6 A geometric model from a planar double-columned infinite ladder to interwoven two double-stranded helical chains through rolling.

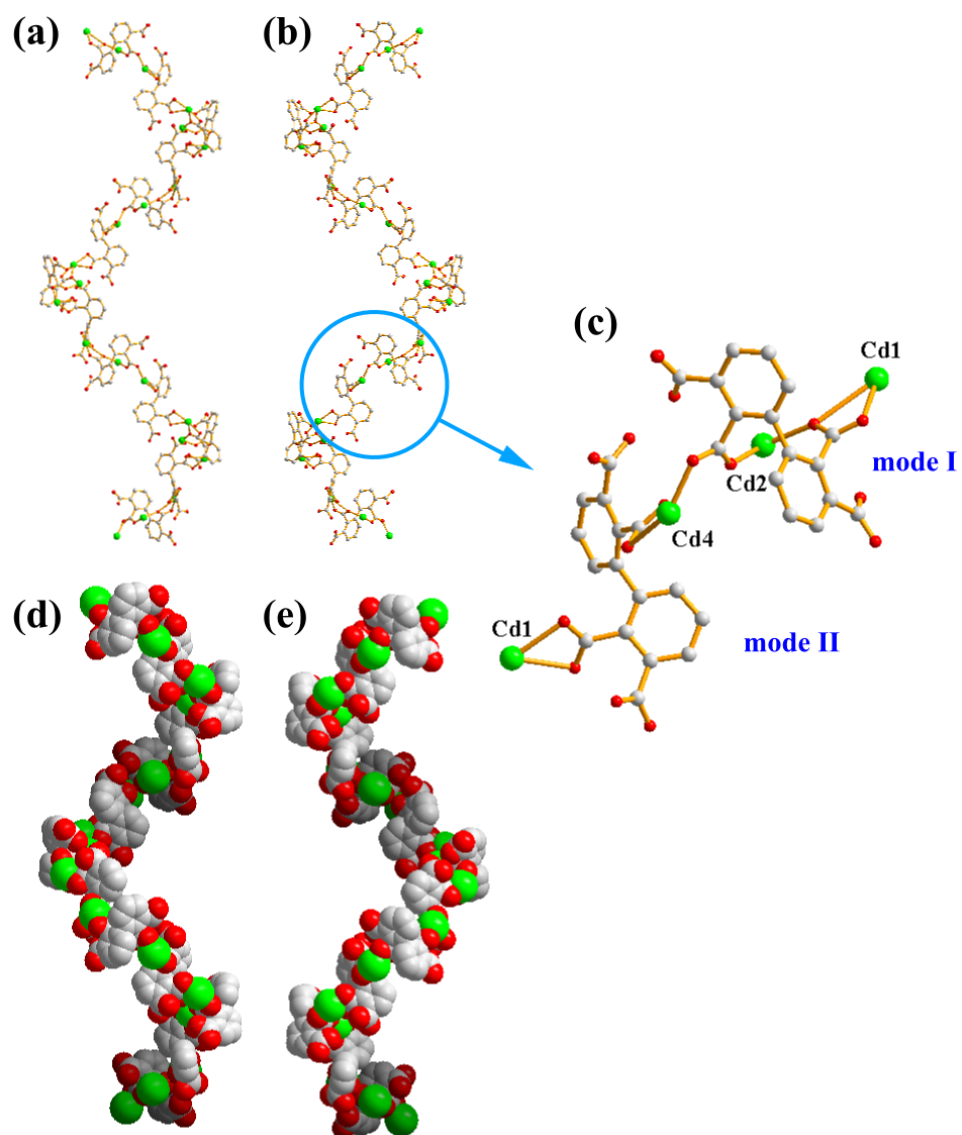


Fig. S7. (a), and (b), Showing the right- and left-handed helical chains in the triple-helical-strand (c), The smallest repeat unit of the right-handed triple-stranded helix (d), and (e), Space filling models of the helical chains showing their quasi-helical ribbon characteristic.

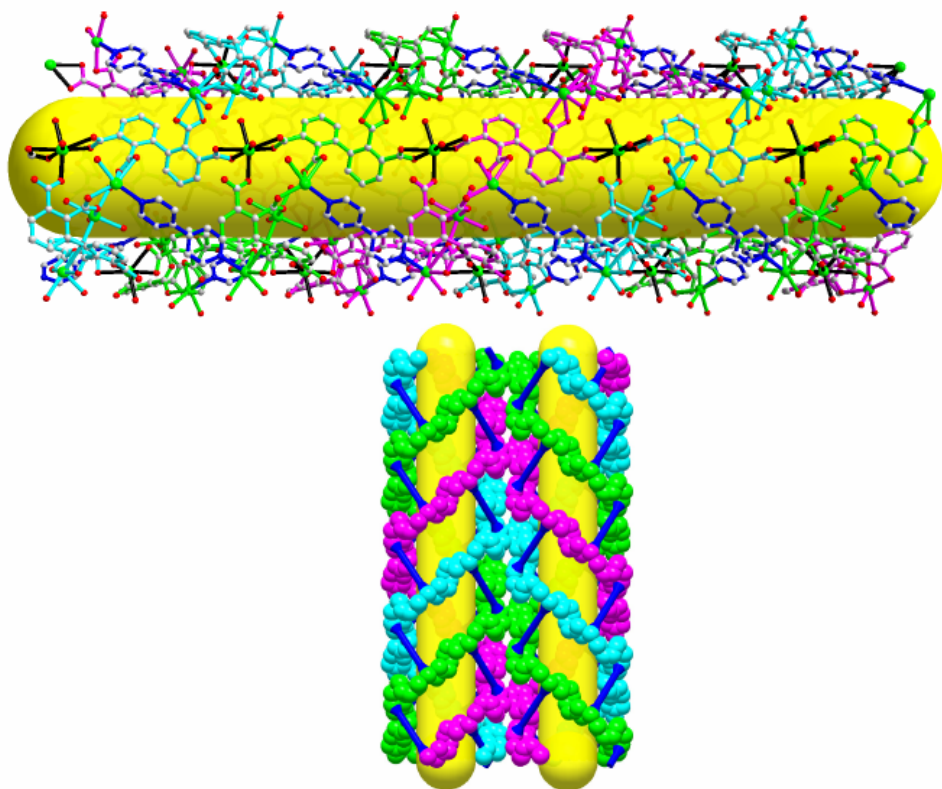


Fig. S8 Top: View of the large helical channel. The triple-helical chains are marked as magenta, cyan, and green. Bpy are marked as blue. Black bonds indicate coordination to Cd₃ ions that connect adjacent chains. Down: Space-filling model represents two adjacent large helical channels with opposite chirality (bpy molecules are represented as blue sticks while Cd₃ ions are omitted).

The same metal centers with the same chirality are coordinated by the coupled ligands, leading to the replication of the conformational chirality from one to other in one helix. Wonderfully, the severely twisted bptc ligands further leads to local chirality in every single chain, giving a *quasi-helical ribbon* arrangement (Fig. S7d, 7e and S9).

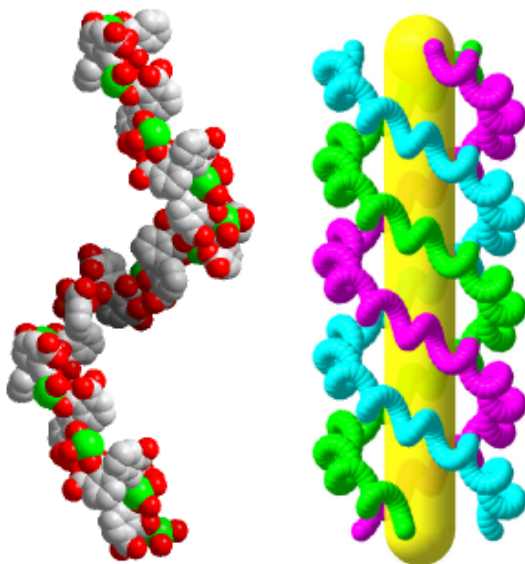


Fig. S9 Lift: one single left-handed helical chain. Right: The simulated triple-stranded quasi-helical ribbons.

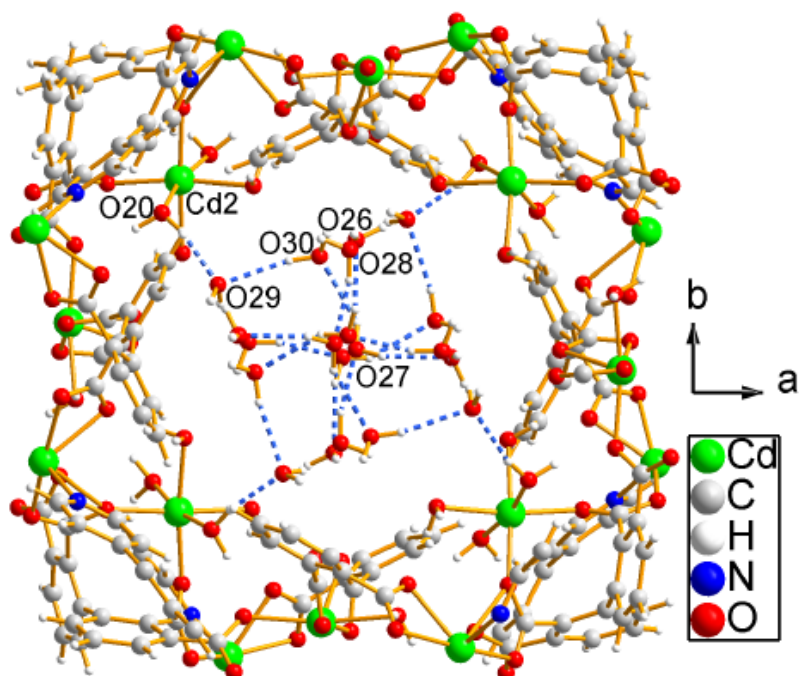


Fig. S10 Solvent water molecule arrangements and hydrogen bonds in the hydrophilic helical channel.

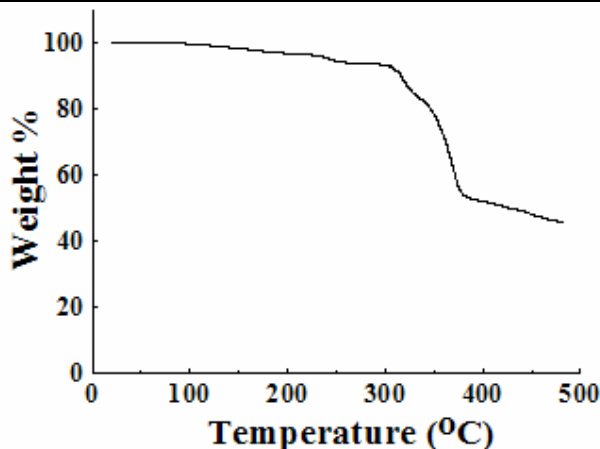


Fig. S11 The TG analysis of **1** revealed that approximately 7.4 % (calcd, 6.6 %) weight is gradually lost in the range of 100-250°C according to the weight lose of solvent waters in the porous ($5.5\text{H}_2\text{O}$ for four Cd atoms). The abrupt weights lose of coordination waters at approximately 300°C gives an undistinguishable step due to the subsequent decompose of the sample. This is reasonable, since the coordination waters play an indispensable role in the formation of framework.

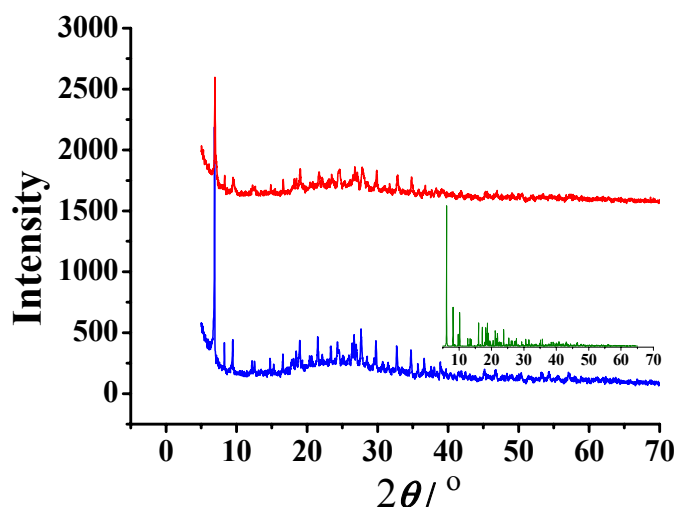


Fig. S12 PXRD patterns for **1**. (bottom) Taken at room temperature (insert: simulated patterns), and (top) after heating to 200°C for two hours.

The positions of the diffraction peaks of the experimental and simulated XRD patterns matched well, indicating phase purity of the as-synthesized sample. Powder X-ray diffractograms of the sample before and after expulsion of solvent waters at about 200°C reveal only minor differences in the diffraction patterns and intensities, which suggests that the integrity of the host lattice is robust to the exclusion of solvent waters. Detailed physical studies about this and several relative interesting frameworks builted from the ligand of H₄bptc and its isomeric are in process and will be reported as a full paper.

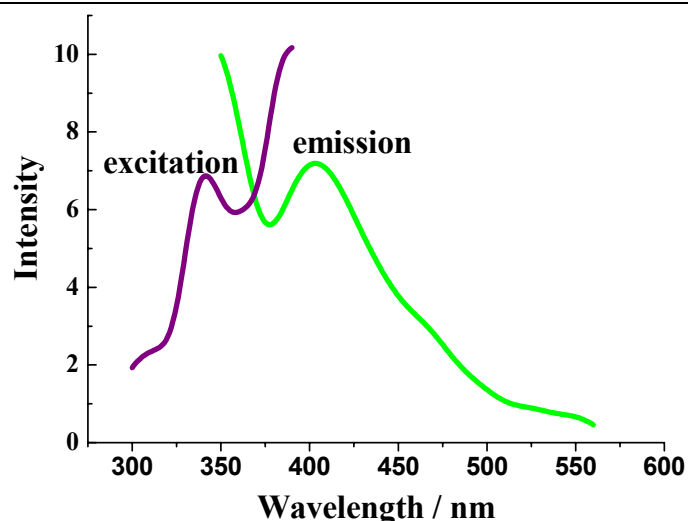


Fig. S13 The excitation and emission spectra of **1**.

To examine the photoluminescent properties of **1**, the luminescence of **1** was investigated. While the free H₄bptc ligand displays very weak luminescence ($\lambda = 390\text{nm}$) in the solid state at room temperature, compound **1** exhibits a distinct radiation emission maximum at $\lambda = 404\text{ nm}$ upon excitation at $\lambda = 340\text{ nm}$ (Fig. S13). The enhancement of luminescence may be attributed to ligand chelation to the metal center, which effectively increases the rigidity of the ligand and reduces the loss of energy by radiationless decay.¹

1. Valeur, B. Molecular Fluorescence: Principles and Application, Wiley-VCH, Weinheim, 2002.